Supplementary Information

Ratiometric Near Infrared Fluorescence Imaging of Dopamine with 1D and 2D nanomaterials

Bjoern Hill[a§], Jennifer M. Mohr[a§], Isabelle K. Sandvoss[a†§], Juliana Gretz[a], Phillip Galonska[a], Lena Schnitzler[a‡], Luise Erpenbeck[b], Sebastian Kruss[a,c]*

[a] *Department of Chemistry, Ruhr Universität Bochum, 44801 Bochum, Germany*

[b] *Department of Dermatology, University Hospital Münster, 48149 Münster, Germany*

[c] *Fraunhofer Institute for Microelectronic Circuits and Systems, 47057 Duisburg, Germany*

[†] *Present Adress: Translational Neuroinflammation and Automated Microscopy, Fraunhofer-Institute for Translational Medicine and Pharmacology, 37075 Göttingen, Germany*

[‡] *Present Adress: Imec the Netherlands, 5656 AE Eindhoven, The Netherlands*

[§] *These authors contributed equally*

** Corresponding author: sebastian.kruss@rub.de*

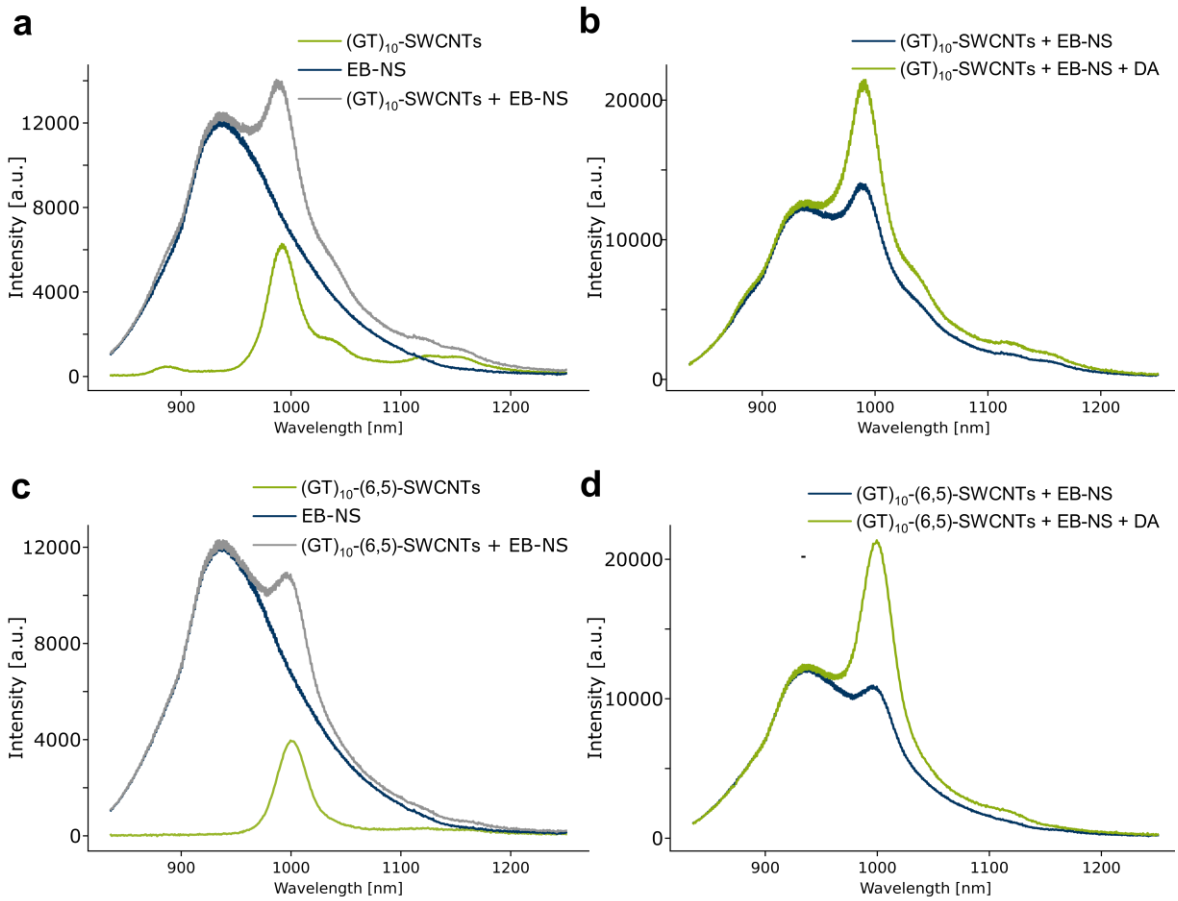

Fig. S1: Simulated ratiometric sensor for candidate NIR-fluorescent nanomaterials. Experimental NIR-fluorescence spectra of different SWCNTs were added to experimental spectra of EB-NS as possible reference. The individual summed spectra are shown in a, c. The effect of dopamine addition to sensor and reference combinations are shown in b, d. Sensor signals (SWCNTs) are shown in blue, references (EB-NS) in orange, summed-up spectra in green and spectra after dopamine addition in magenta. The spectra were calculated using Python. The results indicate that monochiral (6,5)-(GT)10-SWCNTs are better suited for a clean ratiometric response than multichiral CoMoCAT-(GT)10-SWCNTs.

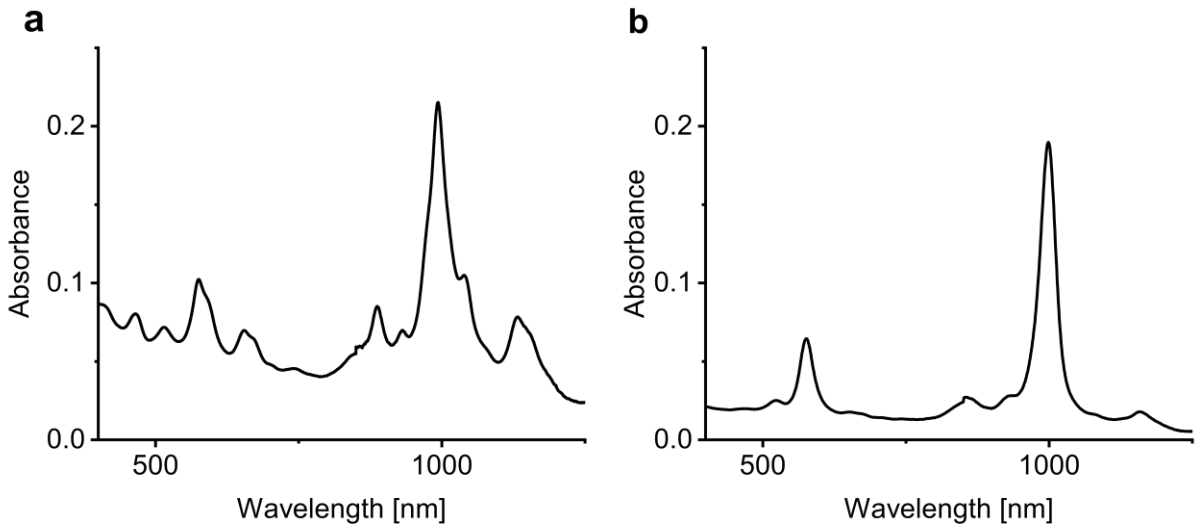

Fig. S2: Absorption spectra of 8.3 nM CoMoCAT-(GT)10-SWCNTs (a) and 2.34 nM (6,5)-(GT)10-SWCNTs (b).

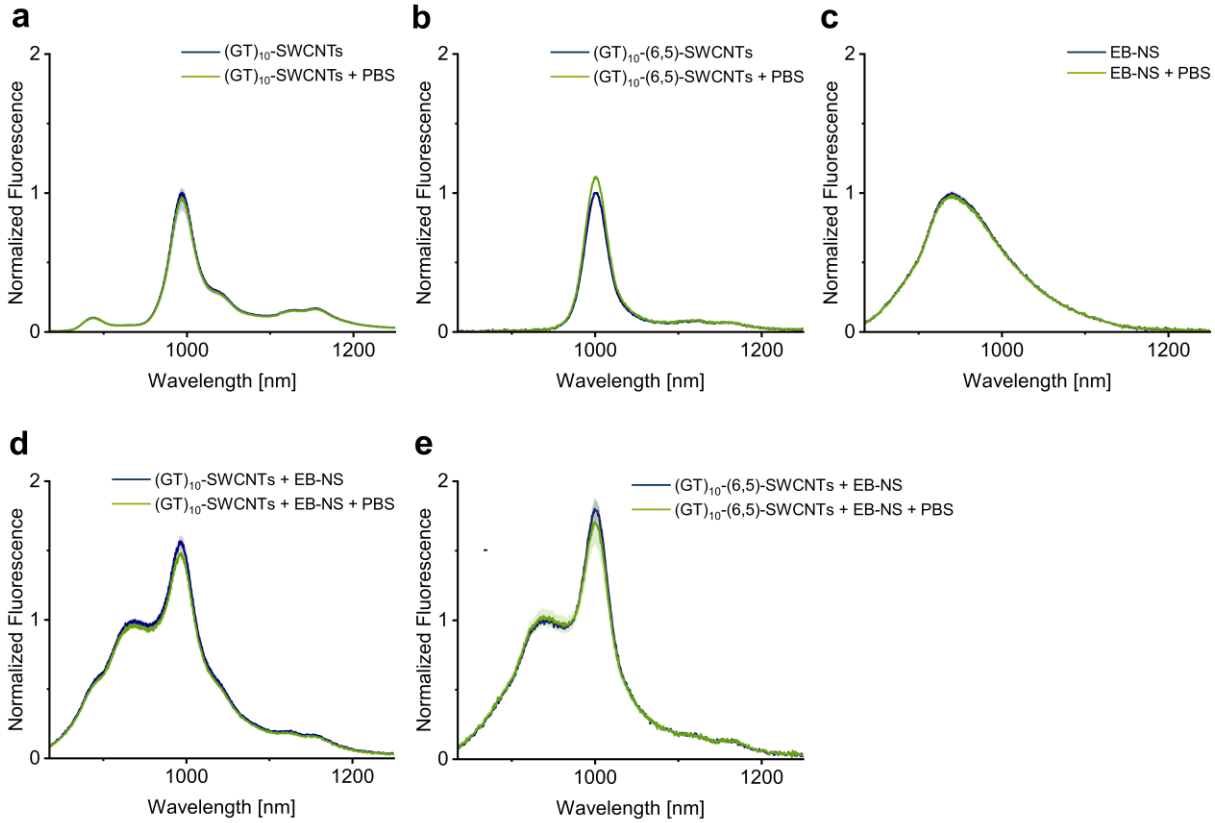

Fig. S3: Control measurements of sensors dispersed in PBS: NIR-fluorescence spectra before and after the addition of 1 x PBS instead of dopamine as a control. Errors shown as shades in spectra = SD (n=3). a) NIR-fluorescence spectra of (GT)10-SWCNTs (0.1 nM). b) NIR-fluorescence spectra of (GT)10-(6,5)-SWCNTs (0.1 nM). c) NIR-fluorescence spectra of EB-NS (0.76 mg/ml). d) NIR-fluorescence spectra of a ratiometric sensor (EB-NS and (GT)10-SWCNTs). e) NIR-fluorescence spectra of a ratiometric sensor (EB-NS and (GT)10-(6,5)-SWCNTs).

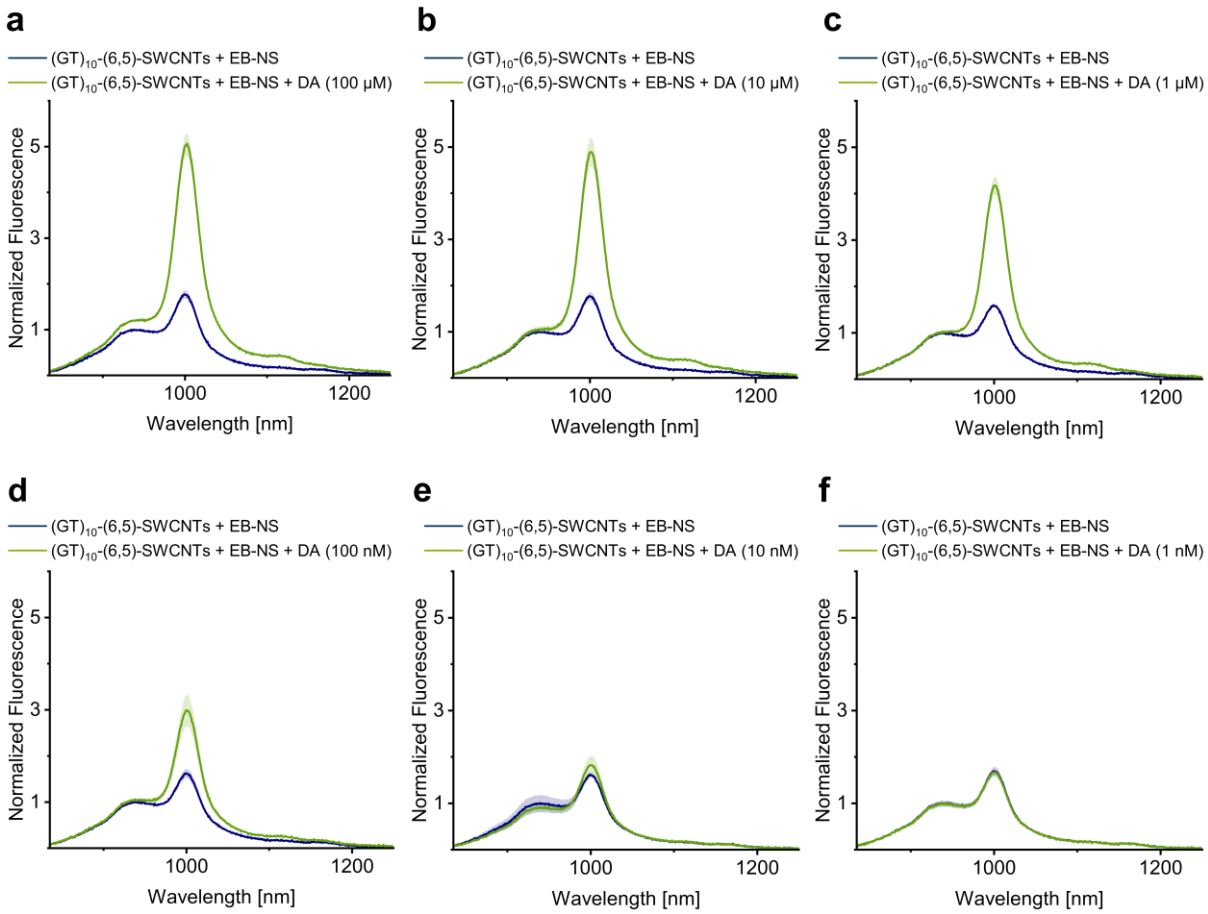

Fig. S4: NIR-fluorescence spectra measured for the calibration curve of the ratiometric dopamine sensor in dispersion in PBS (0.1 nM (6,5)-(GT)10-SWCNTs, 0.76 mg/ml EB-NS). Shown are spectra before and after the addition of dopamine (DA) to different end concentrations: 100 µM (a), 10 µM (b), 1 µM (c), 100 nM (d), 10 nM (e), 1 nm (f). Blue shows the spectra before and green the spectra after the addition of dopamine. Errors shown as shades = SD (n=3).

Table T1: Fit Parameters to the calibration curve shown in figure 2f.

Model	Hill
Equation	y=Vmax*x^n/(k^n+x^n)
Vmax	1.77276 ± 0.06247
k	1.19547E-7 ± 2.95187E-8
n	1.0952 ± 0.13843
R^2	0.99861

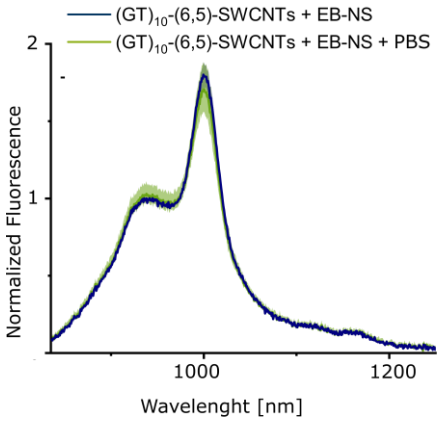

Fig. S5: Ratiometric response on surfaces: NIR-fluorescence spectra of the adsorbed components of the ratiometric sensor before and after the addition of PBS as a control to the addition of dopamine. Errors shown as shades in spectra = SD (n=3).

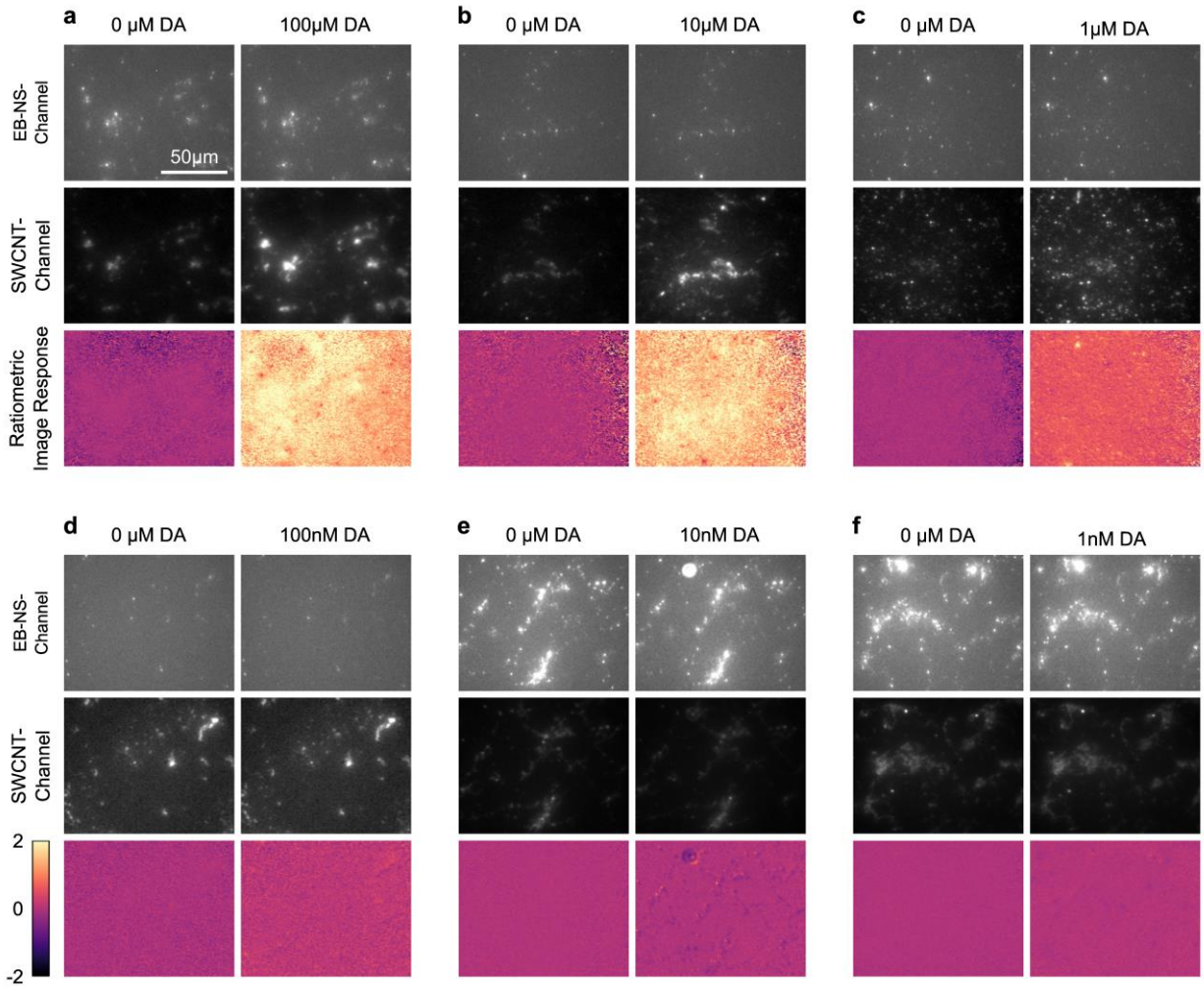

Fig. S6: Fluorescence microscopy images and ratiometric image response measured for the calibration curve of the ratiometric dopamine sensor adsorbed on surface. Shown are the ratiometric image responses before and after the addition of dopamine (DA) at different end concentrations: 100 µM (a), 10 µM (b), 1 µM (c), 100 nM (d), 10 nM (e), 1 nm (f). The scale bar is representative for all shown images.

Table T2: Fit Parameters to the calibration curve shown in figure 3b.

Model	Hill
Equation	y=Vmax*x^n/(k^n+x^n)
Vmax	1.77225 ± 0.02869
k	1.111399E-6 ± 7.82203E-8
n	1.07438 ± 0.08321
R^2	0.9993

The ratiometric response upon addition of 10^{-4} M was not included in the fit due to dopamine polymerization.

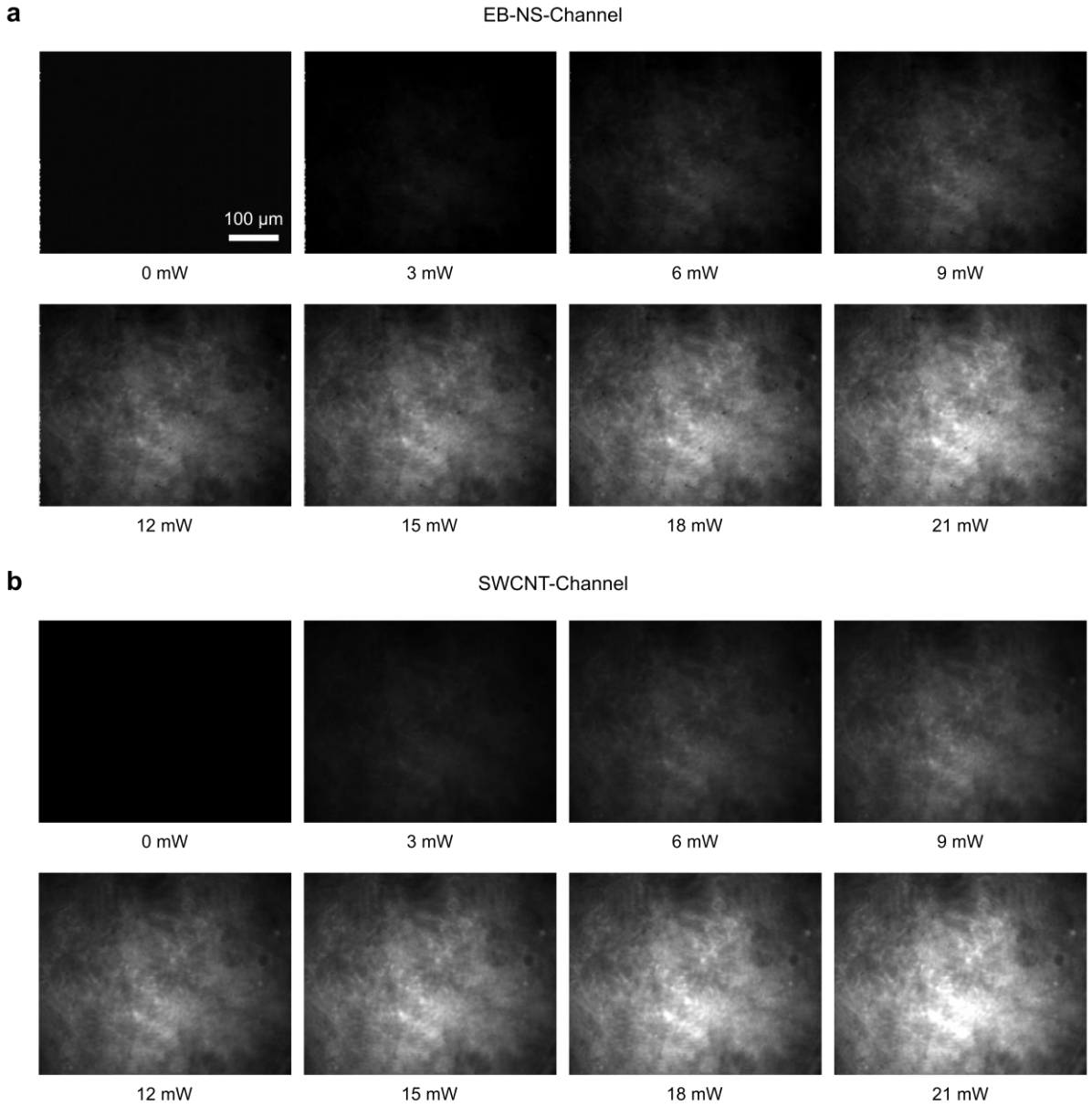

Fig. S7: Fluorescence microscopy images of the ratiometric sensor adsorbed on glass surfaces for varying excitation powers without the addition of dopamine corresponding to the data in Figure 4a. The scale bar is representative for all shown images.

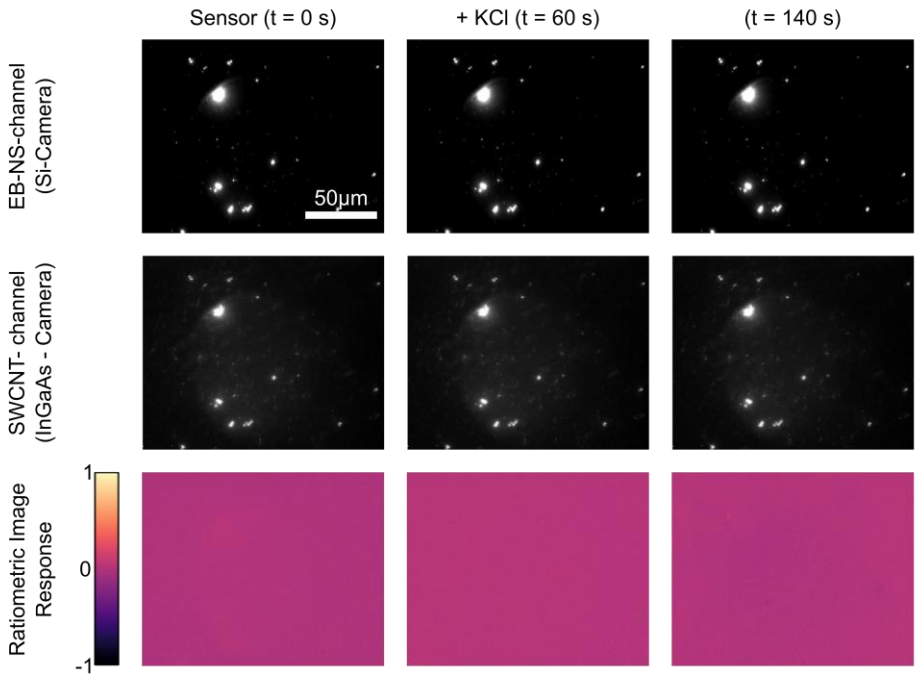

Fig. S8: Fluorescence microscopy images of the sensor with EB-NS and (GT)10–(6,5)-SWCNTs over a time course of 140 s with 100 mM KCl addition at 60 s as a control to the cell experiments on both Si-Camera for EB-NS detection, InGaAs-Camera for SWCNT detection and the resulting ratiometric image response. It shows the superior photostability of the materials. The scale bar is representative for all shown images.

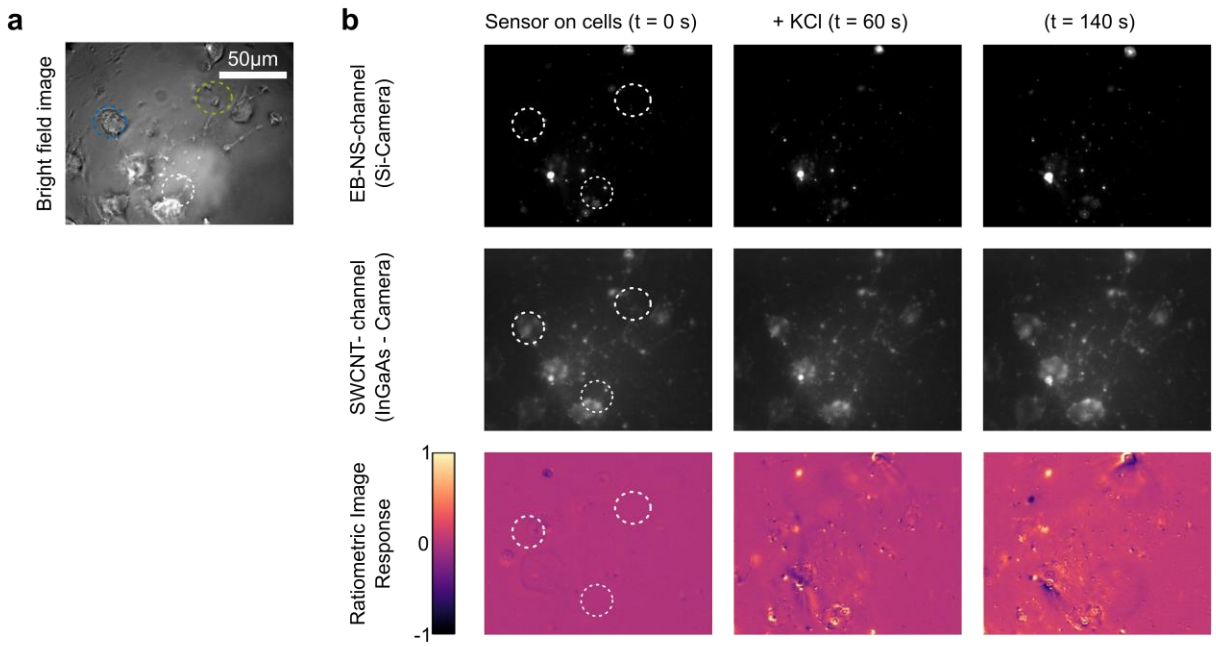

Fig. S9: Additional ratiometric NIR imaging of dopamine release from neuronal cells. a) Brightfield image of differentiated Neuro 2a cells in HBSS with 2 mM CaCl2. Three exemplary regions of interest are marked by dashed circles. b) Corresponding fluorescence images of EB-NS, SWCNTs and the resulting ratiometric response.

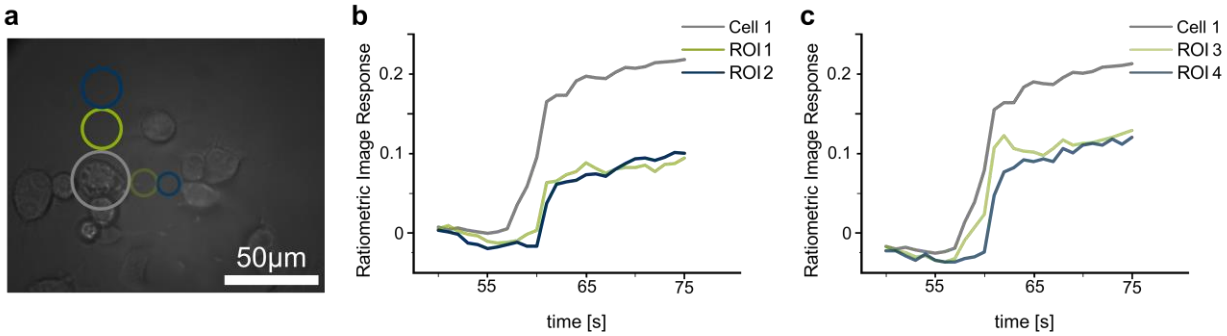

Fig. S10: Dopamine diffusion. a) Bright field image of differentiated Neuro 2a cells in HBSS with 2 mM CaCl2. b) Ratiometric image response of the ROI around the cell and 2 areas to the right with increasing distance from the cell show an increase after the addition of 100 mM KCl. The intensity increase diminishes progressively across the three ROIs, becoming slower as the distance from the cell increases. c) Ratiometric image response of the ROI around the cell and 2 areas to the right with increasing distance from the cell show an increase after the addition of 100 mM KCl. The intensity increase diminishes progressively across the three ROIs, becoming slower as the distance from the cell increases.